An Integrated Analysis of Spherical Aerosol distribution in Eastern Asia based on Ground/Space-based Lidar and A Chemical transport model

Yukari HARA[1], Itsushi UNO[2], Atsushi SHIMIZU[1], Nobuo SUGIMOTO[1], Ichiro MATSUI[1], Jun-ichi KUROKAWA[1], Toshimasa OHARA[1], Zhaoyan LIU[3], Yuanhang ZHANG[4], Xingang LIU[4], Zifa WANG[5]

[1] *National Institute for Environmental Studies, 16-2 Onogawa, Tsukuba, 305-8506, Japan,*
E-mail: hara.yukari@nies.go.jp
[2] *Kyushu University, 6-1 Kasugakouen, Kasuga, 816-8580, Japan*
[3] *National Institute of Aerospace, Hampton, VA 23666, USA*
[4] *School of Environment, Beijing Normal University, Beijing, P.R.China, 100875*
[5] *Institute of Atmospheric Physics, Beijing, China*

ABSTRACT

Seasonal variation of spherical aerosol distribution in East Asia was investigated based on ground/space-based Lidar measurements and Community Multi-scale Air Quality Modeling System (CMAQ) chemical transport model simulation during July 2006 – December 2008. The model results successfully capture the observed typical seasonal variation of Asian spherical aerosols at four NIES lidar sites surrounding East China Sea (Beijing, Guangzhou, Seoul, Hedo/Okinawa). Integrated results of NIES lidar and the chemical model show that a critical composition difference exists among lidar sites; especially, various aerosols exist at Beijing with 25% of dust and 75% of spherical aerosols composed by 20% of carbonaceous aerosol and 80% of sulfate in annual average. The integrated result also showed that seasonal variation pattern of spherical AOT can be classified into 'summer peak' type like that at Beijing and 'summer trough' type, like that at Hedo/Okinawa. The two-month mean horizontal distribution of spherical extinction coefficient indicates that Asian summer/winter monsoon system contributes strongly to the seasonal variation of spherical aerosol; the westerly winter monsoon dilutes the polluted air intensively, the concentration level at high latitude is low in winter. In summer, southern summer monsoon transports pollutants northward. The AOT level at higher continental latitudes increases significantly.

1. INTRODUCTION

The Asian aerosol effects on public health and regional/global climate system are complex and strong because of various anthropogenic and natural compositions. Menon et al. (2002) [1] demonstrated, based on a model study, that absorption of anthropogenic aerosols is a contributing factor to the observed "northern drought with southern flooding" phenomenon in China [2], thereby altering regional atmospheric circulation. Field experiments are very important to understand the interaction between Asian aerosols and regional climate systems. Several international field campaigns have been conducted to elucidate pollutant gases, aerosols characteristics, and radiative forcing in eastern Asia, including ACE-Asia, TRACE-P, EAREX 2005 [3, 4, 5]. These experiments provided beneficial information related to aerosol chemical and physical characteristics and transport structures through integration of field measurements and model studies. However, they were conducted mainly during a single season. The seasonal variation of aerosols distribution has not been clarified well yet.

Since 2001, the National Institute for Environmental Studies (NIES) has been constructing ground-based lidar networks with automated dual wavelength / polarization Mie-lidar systems to observe air quality in the Asian region [6]. From June 2006, space-borne backscatter lidar, Cloud–Aerosol Lidar with Orthogonal Polarization (CALIOP), onboard NASA/CALIPSO satellite, has been measuring global aerosol and cloud vertical distributions continuously with very high spatial resolution [7]. As described in this paper, we present the seasonal variation of aerosol distribution in eastern Asia based on NIES lidar network observations, the Community Multi-scale Air Quality Modeling System (CMAQ) chemical transport model, and CALIOP observations during July 2006 – December 2008.

2. CHEMICAL TRANSPORT MODEL

Transport of air pollutants was simulated using Community Multi-scale Air Quality (CMAQ) ver. 4.4

modeling system released by the US EPA [8]. The Statewide Air Pollution Research Center ver. 99 (SAPRC-99) chemical mechanism for gas phase chemistry, and the AERO3 module for aerosol calculation were used. Anthropogenic emissions were obtained from the Regional Emission Inventory in Asia (REAS) [9]. The horizontal model domain is 6240 × 5400 km^2 on rotated polar stereographic map projection centered at 25 °N, 115 °E with 80 × 80 km^2 grid resolution (see Figure 1). The vertical resolution is stretching 14 layers against the hybrid sigma-z coordination up to z=23 km, which has seven layers within the boundary layer less than 2 km. We conducted two numerical experiments based on different emission scenario. The first one includes all anthropogenic emission for the base year 2005 of REAS emission inventory (CNTL). The other assumes that anthropogenic emissions from China are all set zero (COFF) in order to evaluate the impact of pollutant emission from China. Detailed CMAQ applications can be found in [10].

3. GROUND/SPACE-BASED MIE LIDAR OBSERVATION SYSTEM

Mie-scatter Lidar is a powerful method for measuring the vertical structure of dust and pollutants [6]. Two and a half year ground/space lidar data were used in this study. We used seven Lidar sites data from the NIES ground-based Lidar network, which provide long-term vertical profiles of aerosols with high spatial and temporal resolution (see Figure 1). The extinction coefficient is derived based on the Fernald's method [11] by setting a boundary condition at 6 km and S1 = 50 sr. Aerosol extinction coefficient is separated into 'dust extinction' and 'spherical particles extinction' using particle depolarization ratio.

For a space-borne Lidar, Level 1B Ver. 2.01 and 2.02 CALIOP data were used. The spherical aerosol extinction coefficient was derived using the forward Fernald's inversion by setting the Lidar ratio S1 = 50 sr. The inversion is started from an altitude of 14 km down to the ground surface. Level 1B Horizontal resolution of 333 m was averaged into 5 km resolution. Level 2's CAD (cloud-aerosol discriminator) data (Ver. 2.01 and 2.02) were used for cloud masking. Details of Lidar data analysis method can be found in [12].

4. RESULTS

First, we validated time variation of CMAQ spherical Aerosol Optical Thickness (AOT) less than 3 km with lidar observations. The spherical extinction coefficient by CMAQ was calculated for black carbon (BC), organic carbon (OC), and sulfate based on [13]. The CALIOP data were monthly averaged under cloud-free conditions if the orbit path was located within the circle

of 100 km distance from the NIES lidar site. Results showed that the present model tends to overestimate or underestimate observed AOT; however, the model reproduced the daily or episodic AOT variation observed by ground-based lidar well. The correlation coefficient between ground-based lidar and CMAQ spherical AOT at NIES lidar sites during two and a half years were significant up to 0.34–0.56 with a 99% confidence level. Although the interannual variation of observed AOT is apparently large, clear seasonal variation of spherical AOT is apparent from both model and observation results. The early summertime (June–Jul.) AOT is larger than that of wintertime (Nov.–Feb.) in Beijing. The CALIOP monthly median AOT also shows a consistent seasonal variation pattern. The AOT at Hedo/Okinawa, a southern Japanese site, has a large value during spring and autumn, but not for summer (Jul.–Aug.).
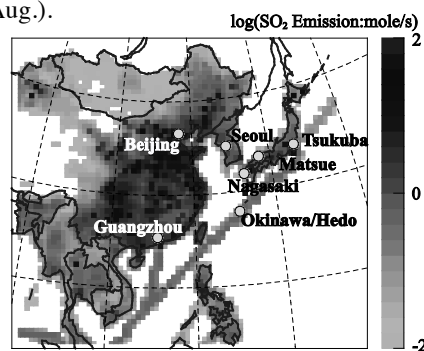

Figure 1. Model domain, distribution of REAS SO2 emission intensity (gray tone level). Circles indicate the locations of NIES LIDAR site; Beijing, Guangzhou, Seoul, Hedo/Okinawa, Nagasaki, Matsue, Tsukuba.

Table 1 presents annual characteristics of spherical AOT at seven NIES lidar sites. The annual mean AOT obtained from NIES lidar measurement decreases gradually from the source to downwind regions, but CMAQ has some difficulty in reproducing this contrast of concentration. It might result from inconsistency of emission and meteorological (e.g. relative humidity) reproducibility. The ratio of carbonaceous to total AOT has the largest value at Beijing, where the ratio of spherical to total AOT has the lowest value, which suggests that various aerosols are mixed, especially at Beijing. On the other hand, AOT at Hedo/Okinawa has the high portion of spherical aerosols composed by sulfate. Finally, AOT ratios showing the emission contribution of China (defined as (AOT$_{CNTL}$ − AOT$_{COFF}$)/AOT$_{CNTL}$) are presented in Table 1. The ratio of 90.5% at Beijing is the highest, suggesting that the AOT level at Beijing is determined almost entirely by that country's own emissions. At Nagasaki and Matsue in Japan, the ratio is around 70%, suggesting a high contribution from China. The ratio of 65% at Hedo/Okinawa is lower than that at either Nagasaki or Matsue, suggesting that AOT at Hedo is affected more

by south Asian emissions. It is clearly shown that a critical difference of aerosol components and emission contribution exists among sites.

To clarify seasonal variation of aerosol vertical profiles, Figure 2 presents two-month averaged vertical profiles of spherical extinction coefficient based on NIES lidar observation (solid lines) at Beijing and Hedo/Okinawa. The AOT and aerosol scale height are also displayed respectively at the bottom and vertical face. Aerosol scale height Z_H is defined as

$$AOT(Z_H) = AOT_{6km}\left(1 - \frac{1}{e}\right),$$

where the total $AOT_{6\ km}$ is calculated the height below z=6 km. From Figure 2, it is apparent that the characteristics of seasonal variation are fundamentally consistent between the model and ground/space-based lidar observations. The aerosol scale height tends to decrease less than 1000 m in wintertime, but it increases to 1500–2300 m during the warm season at Beijing. The seasonal variation of aerosol scale height at Beijing is the largest (about 1 km) among seven lidar sites because of the large seasonal variation of the mixing layer depth (not shown). We can classify typical seasonal variations of spherical AOT at the lidar sites into two types: the 'summertime peak' type and the 'summertime trough' type. Northern sites are apparently belong to the 'summertime peak' type, although southern sites belong to 'summertime trough' type. These seasonal characteristics can be understood by the seasonal variation of spherical aerosols in horizontal distribution. The exchange of air mass between summertime and wintertime strongly affects the seasonal variation of spherical aerosol at each site. Finally, Figure 3 portrays eastern Asian distributions of spherical extinction coefficient averaged for a Jul.-Aug. two month period. Colors show the CALIOP seasonal averaged extinction coefficient. Solid lines show that of CMAQ. The CALIOP data were averaged into grid resolution of 2° (latitude) by 2° (longitude).
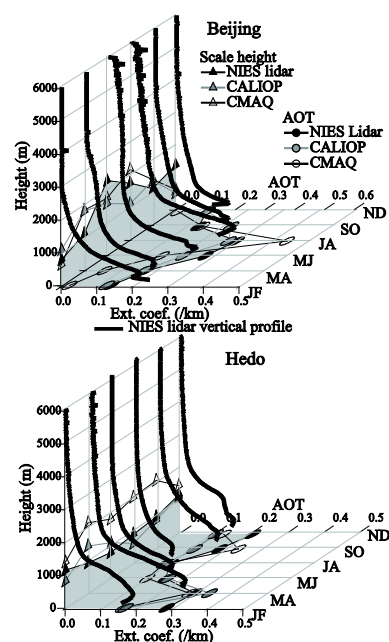

Figure 2. Two-month-averaged vertical profiles of spherical extinction coefficients of NIES Lidar observation (vertical solid lines). AOT in horizontal plane (circles) and aerosol scale height in vertical plane (triangles) based on NIES Lidar (black), CALIOP (gray), and CMAQ (open markers).
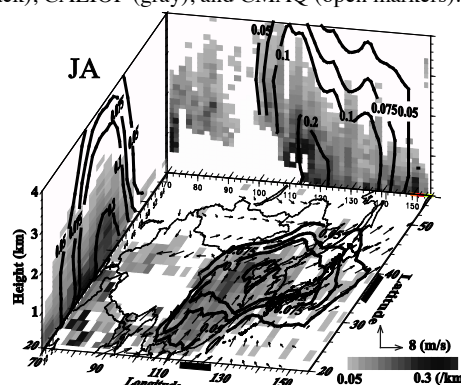

Figure 3 Jul.-Aug.-averaged 3-D seasonal distributions of spherical extinction coefficients less than 3 km height for CALIOP (color) and CMAQ (contour). The latitudinal cross section is averaged for 110–115°E. The longitudinal cross section is averaged for 35–40°N. Wind vectors less than 3 km height level.

Table 1. Annual characteristics of spherical AOT at NIES lidar sites

	Beijing	Guang-zhou	Seoul	Hedo	Nagasaki	Matsue	Tsukuba
Longitude (°E)	116.37	113.26	126.95	128.25	129.98	133.01	140.12
Latitute (°N)	39.97	23.13	37.46	26.87	32.94	35.48	36.05
sphere/total AOT ratio (%) [a]	74.8	86.8	91.6	90.0	86.6	78.8	83.7
Sphere AOT [a]	0.212	0.274	0.164	0.135	0.097	0.104	0.076
CMAQ AOT [b]	0.144	0.182	0.215	0.112	0.162	0.180	0.136
Sulfate AOT fraction (%) [b]	78.7	84.5	80.6	91.5	89.0	88.6	88.7
Carboneous aerosol AOT fraction (%) [b]	21.3	15.5	19.4	8.5	11.0	11.4	11.3
$(AOT_{CNTL}-AOT_{COFF})/AOT_{CNTL}$ (%) [c]	90.5	80.8	66.6	64.9	69.2	68.8	51.5

a Values derived from ground-based Lidar measurement.
b Values derived from CMAQ model simulation.
c Sensitivity of AOT fraction from Chinese emission

From this composite analysis, the seasonal variations of transport pathway and spherical aerosol layer thickness are shown clearly. In summer (Jul.–Aug.), the maritime air mass penetrates from the south. Consequently, the AOT level over southern areas (e.g., Hedo and Guangzhou) decreases because of the coverage of a clean Pacific air mass. On the other hand, as shown in Figure 2, the AOT level over northeastern China increases because of the northward transport of pollutant from high concentration region and weak surface winds. The seasonal mean surface wind speed is lowest in Jul.–Aug. at Beijing (3.8 m/s). The latitudinal cross-section of extinction coefficient averaged from 110–115°E shows that the aerosol layer depth increases gradually from the cold season to the warm season, although CMAQ tends to overestimate the aerosol layer thickness. Latitudinal and longitudinal cross sections also show a northward shift of the anthropogenic aerosol plume attributed to the summer monsoon. Even though, the CMAQ results tend to overestimate aerosol thickness, typical seasonal variation patterns are fundamentally consistent between CMAQ and CALIOP observations. We confirm that the seasonal variations of spherical aerosols observed by ground/space-based Lidar are well explained and correlated by the seasonal exchange of the Asian summer/winter monsoon.

5. CONCLUSIONS

Seasonal variation of spherical aerosol in eastern Asia was analyzed using ground/space-based lidar measurements and the Community Multi-scale Air Quality Modeling System (CMAQ) chemical transport model during July 2006 – December 2008. Based on the model results and lidar observations at four NIES lidar sites surrounding the East China Sea, results show that model results capture the typical seasonal variation of Asian spherical aerosols at NIES lidar sites. We can classify the seasonal variation of spherical AOT at the lidar sites into two typical patterns: the 'summertime peak' type like that at Beijing and Seoul, and the 'summertime trough' type, like that at Guangzhou and Hedo/Okinawa. From the horizontal distribution of spherical aerosols based on CMAQ and CALIOP, seasonal variations of spherical aerosols observed by lidar are explained well by seasonal variations of Asian summer/winter monsoon system.

REFERENCES.

[1] Menon, S., J. Hansen, L. Nazarenko, and Y. Luo, 2002: Climate effects of black carbon aerosols in China and India, *Science*, **297**, 2250–2253, doi:10.1126/science.1075159.

[2] Xu, Q., 2001: Abrupt change of the mid-summer climate in central east China by the influence of atmospheric pollution, *Atmos. Environ.*, **35**, 5029–5040, doi:10.1016/S1352–2310(01)00315–6.

[3] Huebert, B. T., T. Bates, P. B. Russell, G. Y. Shi, Y. J. Kim, K. Kawamura, G. Carmichael, and T. Nakajima, 2003: An overview of ACE-Asia: Strategies for quantifying the relationships between Asian aerosols and their climatic impacts, *J. Geophys. Res.*, **108**(D23), 8633, doi:10.1029/2003JD003550.

[4] Jacob, D. J., J. H. Crawford, M. M. Kleb, V. E. Connors, R. J. Bendura, J. L. Raper, G. W. Sachse, and J. C. Gille, 2003: The Transport and Chemical Evolution over the Pacific (TRACE-P) aircraft mission: Design, execution, and first results, *J. Geophys. Res.*, **108**(D20), 9000, doi:10.1029/2002JD003276.

[5] Ramanathan, V. and P. J. Crutzen, 2003: New directions: Atmospheric brown clouds, *Atmos. Environ.*, **37**, 4033–4035.

[6] Shimizu, A., N. Sugimoto, I. Matsui, et al., 2004: Continuous observations of Asian dust and other aerosols by polarization lidars in China and Japan during ACE-Asia, *Journal of Geophysical Research*, **109**, D19S17.

[7] Winker, D. M., W. H. Hunt, and M. J. McGill, 2007: nitial performance assessment of CALIOP, *Geophys. Res. Lett.*, **34**, L19803.

[8] Byun, D. W., and J. K. S. Ching, 1999: Science algorithms of the EPA Models-3 community multi-scale air quality (CMAQ) modeling system, NERL, Research Triangle Park, NC EPA/ 600/R-99/030.

[9] Ohara, T., H. Akimoto, J. Kurokawa et al., 2007: Asian emission inventory for anthropogenic emission sources during the period 1980–2020, *Atmos. Chem. Phys.*, **7**, 4419–4444.

[10] Uno, I., et al., 2007: Systematic analysis of interannual and seasonal variation of model-simulated tropospheric NO2 in Asia and comparison with GIME-satellite data, *Atmos. Chem. Phys.*, **7**, 1671–1681.

[11] Fernald, F. G., 1984: Analysis of atmospheric LIDAR observations: Some comments, *Appl. Opt.*, **23**, pp. 652-653.

[12] Hara, Y., K. Yumimoto, I. Uno et al., 2009: Asian Dust Outflow in the PBL and Free Atmosphere retrieved by NASA CALIPSO and an assimilated Dust Transport Model, *Atmos. Chem. Phys.*, **9**, 1229–1239.

[13] Takemura, T., H. Okamoto, Y. Maruyama, A. Numaguti, A. Higurashi, and T. Nakajima, 2000: Global three-dimensional simulation of aerosol optical thickness distribution of various origins, *J. Geophys. Res.*, **105**, 17,853–17,873.